The Journal of Experimental Biology 203, 3189–3198 (2000)
Printed in Great Britain © The Company of Biologists Limited 2000
JEB2955

K^+ CURRENTS IN CULTURED NEURONES FROM A POLYCLAD FLATWORM

STEVEN D. BUCKINGHAM AND ANDREW N. SPENCER*
Bamfield Marine Station, Bamfield, British Columbia, Canada V0R 1B0
*Author for correspondence (e-mail: aspencer@bms.bc.ca)

Accepted 13 July; published on WWW 26 September 2000

Summary

Cells from the brain of the polyclad flatworm *Notoplana atomata* were dispersed and maintained in primary culture for up to 3 weeks. Whole-cell patch-clamp of presumed neurones revealed outwardly directed K^+ currents that comprised, in varying proportions, a rapidly activating (time constant τ=0.94±0.79 ms; *N*=15) and inactivating (τ=26.1±1.9 ms; *N*=22) current and a second current that also activated rapidly (τ=1.1±0.2 ms; *N*=9) (means ± S.E.M.) but did not inactivate within 100 ms. Both current types activated over similar voltage ranges. Activation and steady-state inactivation overlap and are markedly rightward-shifted compared with most *Shaker*-like currents (half-activation of 16.9±1.9 mV, *N*=7, half-inactivation of −35.4±3.0 mV, *N*=5). Recovery from inactivation was rapid (50±2.5 ms at −90 mV). Both currents were unaffected by tetraethylammonium (25 mmol l^{-1}), whereas 4-aminopyridine (10 mmol l^{-1}) selectively blocked the inactivating current. The rapidly inactivating current, like cloned K^+ channels from cnidarians and certain cloned K^+ channels from molluscs and the Kv3 family of vertebrate channels, differed from most A-type K^+ currents reported to date. These findings suggest that K^+ currents in *Notoplana atomata* play novel roles in shaping excitability properties.

Key words: Platyhelminthes, Polycladida, *Notoplana atomata*, K^+ channel, neuronal culture, evolution, *Shaker*, Kv3, whole-cell patch-clamp.

Introduction

The flatworms (Platyhelminthes) occupy a critical position in metazoan phylogeny as they are deeply rooted in the lineage that leads to most, if not all, phyla of bilateral animals (Valentine et al., 1999). Despite this, little is known about their cellular neurophysiology. According to most phylogenetic reconstructions, modern flatworms are expected to resemble the common ancestors of the protostomes and deuterostomes, and should retain some ancestral features that are common to both. The considerable phylogenetic distance between the flatworms and the eubilaterians (Field et al., 1988; Katayama et al., 1996; Turbeville et al., 1992) suggests that a comparison of the structural and functional plesiomorphic features of their nervous systems may expose fundamental structural motifs, with attendant functional properties, that are masked in higher taxa by accumulated selected characteristics. Identification of these fundamental motifs may provide novel insights into structural correlates of function in the more derived channels in the vertebrates.

Voltage-gated K^+ channels play a central role in the control of neuronal excitability (Hille, 1992). What is known to date about voltage-gated K^+ channels of basal phyla confirms that they display considerable diversity in fundamental design. Jellyfish K^+ channels, for example, appear to possess novel features of voltage sensitivity and inactivation (Grigoriev et al., 1997, 1999a–c; Jegla et al., 1995).

Here, we describe the culture of central neurones from *Notoplana atomata* and the recording of voltage-gated K^+ channels from these cells using the whole-cell, patch-clamp technique. *Notoplana atomata* is a polyclad genus for which detailed extracellular and intracellular data are available (Faisst et al., 1980; Keenan and Koopowitz, 1984; Keenan et al., 1979; Koopowitz et al., 1975, 1976, 1979a,b). No voltage-clamp recordings of ionic currents from the neurones of polyclads have been reported. The polyclads are free-living turbellarians and the most basal of the Platyhelminthes, except for the acoels (whose placement within the Platyhelmithes has been challenged; Ruiz-Trillo et al., 1999) and the catenulids, which form a sister group to the rest of the Bilateria (Carranza et al., 1997). The only K^+ channel cloned from platyhelminths is from the parasitic trematode *Schistosoma mansoni* (Kim et al., 1995), and the only description of K^+ currents in platyhelminths is for dispersed muscle cells of *Schistosoma mansoni* (Day et al., 1993) and for cultured neurones of the triclad *Bdelloura candida* (Blair and Anderson, 1993). We show that K^+ currents of *Notoplana atomata* are extremely rightward-shifted, suggesting the extant occurrence of a class of comparatively voltage-insensitive, voltage-gated K^+ channels in the Cnidaria, Platyhelminthes, Annelida and Mollusca, which functionally resemble the unusual Kv3 class of vertebrate *Shaker*-like channels.

Materials and methods

Collection and care of animals

Notoplana atomata (0.5–3 cm) were collected from the underside of rocks in the intertidal zone near Bamfield Marine Station, Bamfield, British Columbia, Canada, and were kept in a glass tank continually supplied with sea water (9–12 °C) from the system at the Station. Animals were used within 3 weeks of capture and fed on brine shrimp.

Cell dissociation and culture

Individuals were anaesthetised by immersion in a 1:1 (v/v) mixture of sea water and 0.33 mol l^{-1} $MgCl_2$ for at least 20 min. They were sterilised by brief immersion in 70 % ethanol, washed in filtered artificial sea water and then pinned out in a Petri dish lined with Sylgard resin. An incision was made in the dorsal epithelium, and the nerves were severed so as to leave fairly long stubs. The brain was removed and placed in a separate Petri dish containing sterile filtered (0.22 μm) artificial sea water. Following longitudinal bisection of the brain with fine scissors, the sheath was removed using two sharpened tungsten needles. The resulting hemiganglia were placed in a solution of 10 mg ml^{-1} pronase in artificial sea water. Teasing the hemiganglia apart with sharpened tungsten needles assisted entry of the enzyme. After approximately 20 min, depending on the rate of dissociation, which varied from preparation to preparation, hemiganglia were rinsed well in several changes of culture medium and transferred to a Petri dish (30 mm, Falcon) containing filtered culture medium (see below) and gently triturated through fire-polished, silanized Pasteur pipettes or glass capillaries. Cultures were incubated at 12 °C for 1–7 days before use in electrophysiological experiments.

Electrophysiological recording

Cells with a cell body diameter of between 40 and 100 μm, and with processes extending for more than twice the cell body diameter, were selected for electrophysiological recording. Cultures were washed several times in artificial sea water (or modified artificial sea water if required by the experiment) and transferred to the stage of a Nikon inverted microscope. Glass pipettes were manufactured from borosilicate glass using a Sutter puller and fire-polished using a Narashige microforge. Pipettes had resistances in the range 300 kΩ to 2 MΩ when filled with the pipette solution described below. These pipettes readily formed seals in the 1–10 GΩ range, and the whole-cell configuration could be obtained by applying negative pressure or a combination of negative pressure and a brief (10–100 ms) pulse of depolarising current. Access resistances were in the range 2–4 MΩ. The cells were voltage-clamped using an Axopatch 1D amplifier, and currents were recorded using the pClamp 6.0 data-acquisition suite (Axon Instruments) running on a Dell Dimension P166v personal computer. Data were analysed using a combination of pClamp 6.02 (Axon Instruments) and SigmaPlot 4.0 (SPSS) analysis software. All recordings were compensated for series resistance by 50–80 % using the feedforward circuit built into the amplifier. Greater compensation could not be used without causing saturation of the feedback amplifier. Thus, a significant voltage error remained in some of our current recordings, which could amount to 20 mV for a 10 nA current after 50 % compensation. The estimated worst-case error is given in the figure legends and in the text where appropriate. Capacitative and leak currents were subtracted on-line using the *P*/*N* protocol provided with the data-acquisition software. *N* inverted copies of the test waveform (the amplitude of each being 1/*N* of the main trial) were applied before each trial. The sum of the currents applied during these prepulses was subtracted from the currents recorded during the main waveform.

Salines and culture media

Salines and pipette-filling solutions were prepared as in Table 1. The volume of 1 mol l^{-1} KOH required to balance the pH was measured to determine the final concentration of K^+. Culture medium consisted of 75 ml of artificial sea water mixed with 25 ml of Leibowitz L-15 culture medium (Sigma, USA) and 50 μg ml^{-1} gentamycin sulphate to which 475 mg of NaCl was added to balance the osmotic pressure to a value approximating that of sea water (approximately 1 osmol l^{-1}).

Results

Cell culture

Dissociated cells adhered readily to untreated plastic Petri dishes. Neurite outgrowth began within 3 h, although some cells had retained neurites through dissociation and trituration. A wide range of cell shapes was seen in culture, including monopolar, bipolar and multipolar cells (Fig. 1), with

Table 1. *Composition of salines and pipette-filling media*

Solution	NaCl (mmol l^{-1})	Choline chloride (mmol l^{-1})	KCl (mmol l^{-1})	$MgCl_2$ (mmol l^{-1})	$CaCl_2$ (mmol l^{-1})	$CoCl_2$ (mmol l^{-1})	Hepes (mmol l^{-1})	EGTA (mmol l^{-1})	pH
ASW	395	–	10	50	10	–	10	–	7.6 (1 mol l^{-1} NaOH)
K-ASW	–	395	10	50	–	10	10	–	7.6 (1 mol l^{-1} KOH)
Pipette	50	–	400	–	1	–	10	11	7.5 (1 mol l^{-1} KOH)
K-pipette	–	51	400	–	–	–	10	–	7.5 (1 mol l^{-1} KOH)

ASW, normal artificial sea water; K-ASW, artificial sea water used for the isolation of K^+ currents; Pipette, normal pipette-filling medium; K-pipette, pipette medium used for the isolation of K^+ currents.

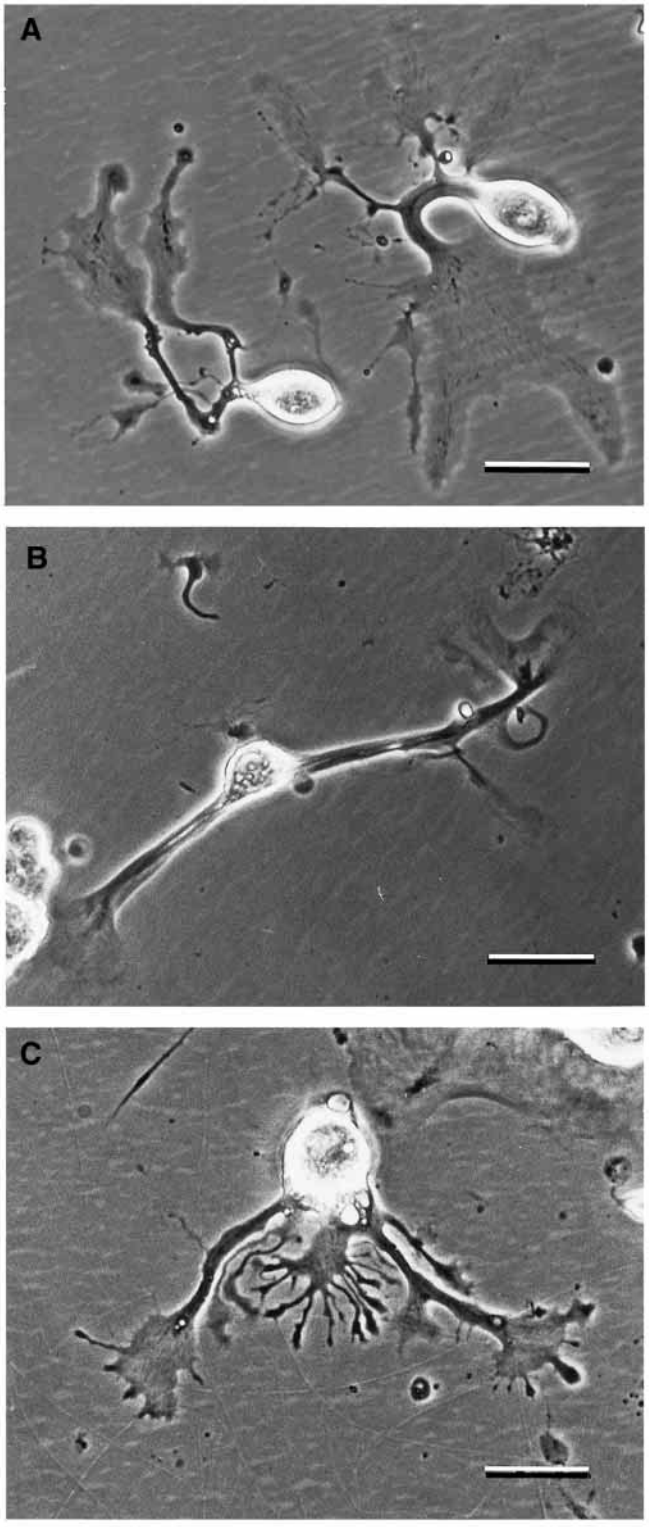

Fig. 1. Dissociated neurones from the brain of *Notoplana atomata* after 44 h in culture. Evidence of neurite regrowth was observed within 3 h of plating. A number of cell shapes were observed, including two variants of monopolar neurones (A) and bipolar (B) and multipolar (C) neurones. Various types of growth cones are seen in these neurones. The neurone at the left in A shows veil-like, lateral extensions of the neurite that are seen in many, but not all, cells. Scale bars, 100 μm.

homopolar and heteropolar examples of these classes. We have assumed that most cells with elongated processes are neurones, although some may be non-neuronal, ensheathing cells.

Cell bodies were 5–100 μm in diameter. Many had aspect ratios near unity, whereas others were distinctly pear-shaped with the cell body merging continuously into the primary neurite. Most neurones had several obvious growth cones. Many neurites were flattened with veil-like lateral extensions (Fig. 1).

Whole-cell currents

The whole-cell, recording configuration could be maintained for 10–30 min. To determine the current–voltage properties of cells in normal artificial sea water (ASW), a series of 100 ms voltage excursions from –90 mV to a range of positive potentials in 10 mV steps was imposed (Fig. 2). In response to a long (>100 ms) test pulse, most cells displayed outward currents that contained both a rapidly inactivating component and a slowly inactivating or non-inactivating component (Fig. 2A), while the remaining neurones expressed only a slowly or non-inactivating outward current (Fig. 2B). These currents were activated above approximately –50 mV. Although most cells produced little or no obvious inward current, 5–10 % of cells gave noticeable, rapid inward currents which reversed above +40 mV (Fig. 2C). These cells all had large cell bodies (capacitance >100 pF) and were difficult to space-clamp. Under current-clamp conditions, these large cells supported overshooting action potentials (Fig. 2D). Not all the cells with cell bodies of this size displayed action potentials.

Inactivating and non-inactivating outward current

Outward currents were activated at potentials above –10 mV (Fig. 3) when Na^+ and Ca^{2+} currents were eliminated using ASW for the isolation of K^+ currents (K-ASW; see Table 1). An inactivating component was present in 83 % of cells (Fig. 3A), whereas only a non-inactivating current was seen in the remaining cells (Fig. 3B). The mean ratio of the peak to steady-state current amplitudes was 2.88±0.47 (N=34) for a 100 ms depolarising step from –90 mV to +80 mV. The distribution of values falling in bins of width 0.5 were counted and found not to differ significantly from a normal distribution (Kolgorov–Smirnov test, P=0.29). Therefore, the ratio of peak to steady-state currents does not provide a criterion by which to classify cells. The difference between the initial and steady-state current amplitudes was not correlated with that of the steady-state current (Pearson product moment, P=0.637). Time to peak decreased slightly with increasing depolarisation from a value of 12.2±3.5 ms (N=18) for steps to 0 mV to 3.0±0.8 ms (N=18) for steps to +80 mV and to 1.37±0.13 ms (N=5) for steps to +130 mV (means ± S.E.M.). The latter two values differ significantly from the first, but not from each other (Kruskal–Wallis one-way analysis of variance on rank, P<0.05). The mean time constant for activation measured from the steep rising phase of responses to depolarising voltage steps to +80 mV was found to be 0.94±0.79 ms (mean ± S.E.M., N=15). When the rapidly inactivating component was isolated

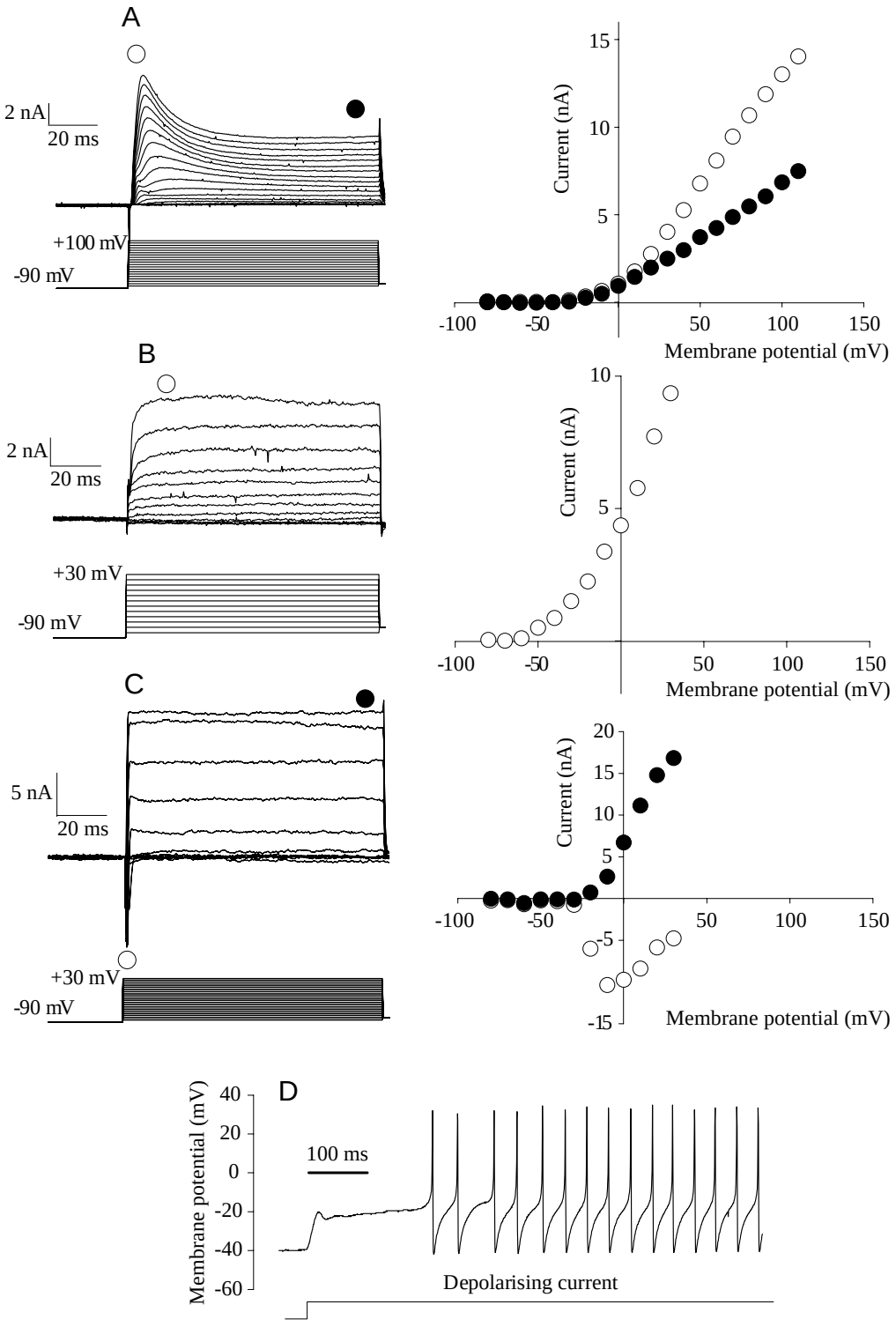

Fig. 2. Whole-cell total currents recorded from cultured neurones in normal artificial sea water. The stimulus protocol is illustrated below the current recordings. Currents were evoked by stepping the membrane potential from a holding potential of –90 mV to a range of potentials from –80 mV to +110 mV (A) or to +30 mV (B,C) in 10 mV increments. Outward current dominated all recordings, with some cells displaying a rapidly inactivating outward current and a slower, sustained outward component (A), whereas other cells showed only the latter component (B). (C) Inward currents and action potentials were evident in some neurones. In normal artificial sea water, a minority of cells (<10 %) displayed a rapidly inactivating inward current in addition to outward currents. The inward current reversed above +40 mV. (D) Cells of the type shown in C, recorded under current-clamp conditions, produced a train of non-adapting, overshooting action potentials upon injection of approximately 10 nA of depolarising current. To the right of each set of traces, current–voltage plots of the data from A, B and C illustrate, respectively, the voltage-dependence of these outward currents at the times indicated by the symbols: open circles, peak current (A,C) or after full activation of the currents (B); filled circles, steady-state current. Symbols placed above the current traces approximate the times at which the corresponding current measurements were made for the current–voltage plots. Maximum estimated voltage errors: A, 20 mV (open circles), 14 mV (filled circles); B, 20 mV; C, 33 mV (filled circles), 20 mV (open circles).

with a conditioning, 100 ms depolarising pre-pulse to +60 mV (Fig. 3C), the time constant of the steep rising phase of the remaining current was 1.10±0.2 ms (mean ± S.E.M., N=9).

Activation

The voltage-dependence of activation of the outward currents was measured in saline containing elevated [K^+] (152 mmol l^{-1}) to enhance tail currents. Cells were stepped to a range of membrane potentials from –80 to +160 mV for 2.5 ms and then returned to a holding potential of –100 mV. Instantaneous tail currents (estimated by fitting the tails to a single exponential and extrapolating back to the end of the activating pulse) were plotted against the value of the depolarising step (Fig. 4). Tail-current amplitudes were all

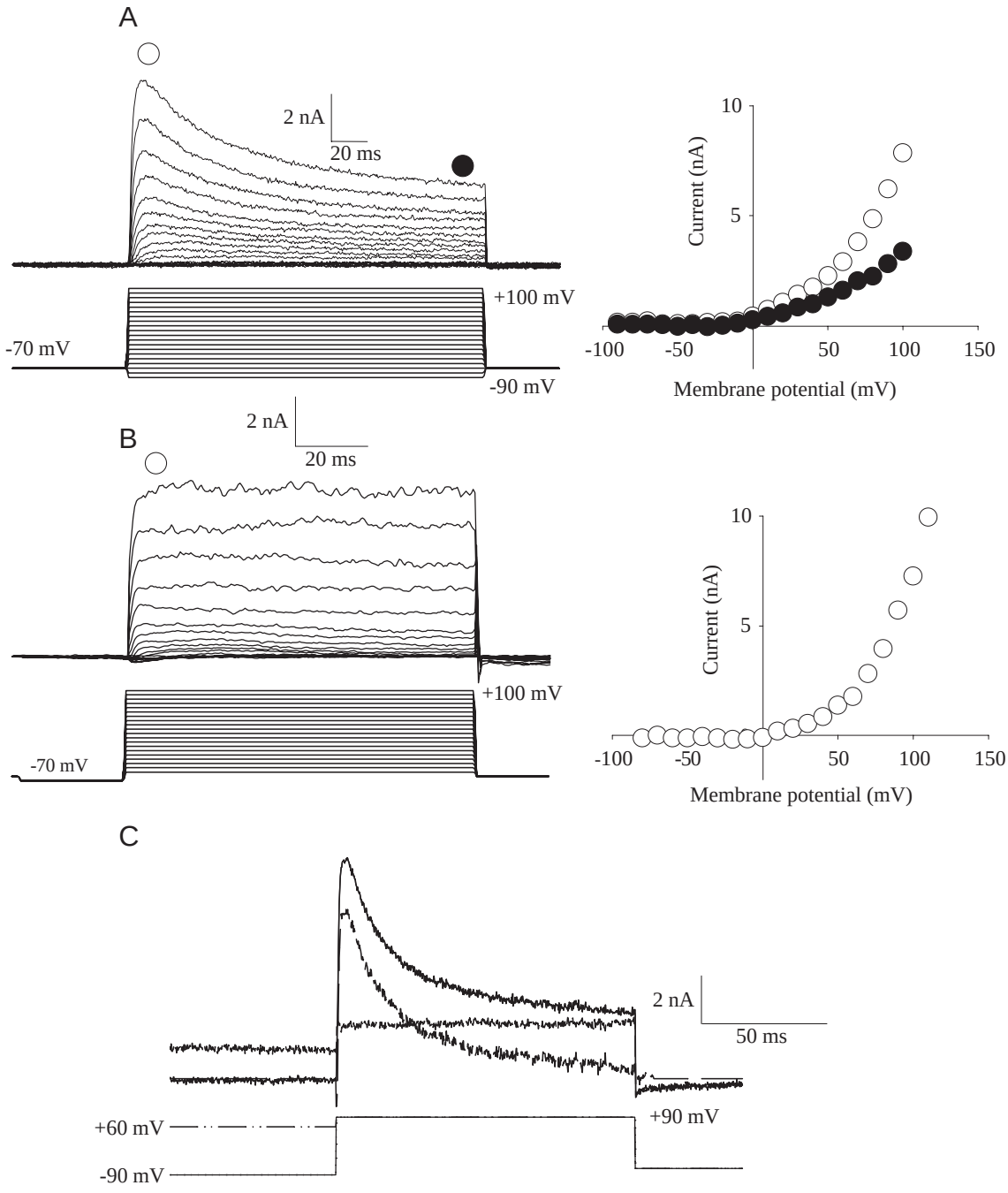

Fig. 3. Whole-cell outward currents recorded in the absence of Na^+ and Ca^{2+} currents. Typical current traces are shown in A and B, with the corresponding current–voltage plots to the right. While some cells possessed both a rapidly inactivating current and a non-inactivating current in various proportions (A), a slow, sustained outward component was present in all cells (B). Currents were evoked by applying voltage steps from a holding potential of –70 mV to potentials ranging from –90 to +100 mV for 100 ms in 10 mV increments. The stimulation protocol is illustrated below the current traces. Artefacts resulting from a slight imbalance in the series resistance compensation were erased. (C) Currents such as those illustrated in A could be resolved into an inactivating and a non-inactivating component by applying a 100 ms prepulse to +60 mV before the series of voltage steps. The inactivating component was then resolved by subtraction of currents evoked using the prepulse from the currents obtained without the prepulse (middle trace). Inactivating and non-inactivating currents have similar thresholds and voltage dependencies. The open circle in A indicates the time at which the measurement of the maximum current was taken, in this case 4 ms after the onset of depolarisation. In B, currents were measured at a time (open circle) corresponding to the time at which peak currents were measured in A. Estimated maximum voltage errors: A, 15 mV (open circles), 6 mV (filled circles); B, 18 mV; C, 22 mV (at peak).

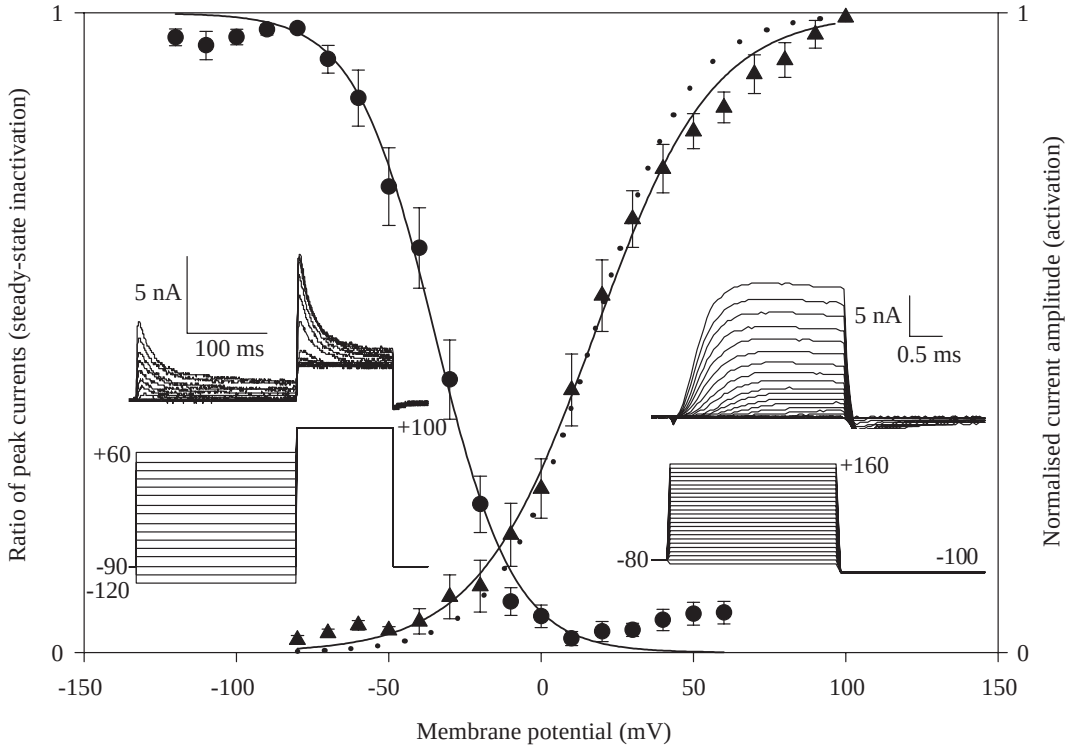

Fig. 4. Activation and inactivation properties of the outward currents. Activation was measured by stepping the membrane potential from a holding potential of −70 mV to a series of values ranging from −80 to +160 mV for 2.5 ms (to activate the currents) and then measuring the tail currents upon return to −100 mV. Instantaneous tail currents were then estimated by fitting the tail currents to a single-exponential function and extrapolating back to the end of the activating pulse (right inset). The amplitudes of the tail currents were normalised and plotted against the values of the test pulse (triangles). Data for individual cells were fitted to a Boltzman function from which the mean half-activation and mean slope were calculated. These parameters were then used to generate a mean Boltzman curve (solid curve). The dotted curve is a fit to the same data, but for which the voltage values had been corrected assuming a maximal series resistance error (4 MΩ and 50 % compensation). Values for half-activation obtained using these approaches were 16.9±1.9 mV, N=6 (dotted line), 17.4±3.9 mV, N=6 (solid line), and 16.4±1.1 mV (triangles) and for slope were 15.0±1.8 mV e^{-1}, N=6 (dotted line), 19.5±3.1 mV e^{-1}, N=6 (solid line), and 18.9±0.8 mV e^{-1} (triangles). Steady-state inactivation was measured using a paired-pulse protocol in which 200 ms depolarising steps from a holding potential of −90 mV to values ranging from −120 mV to +60 mV in 10 mV increments were followed immediately with a step to +70 mV or +100 mV for 120 ms (left inset). The amplitude of the rapidly inactivating component was measured after subtraction of the slowly or non-inactivating component, assuming that full inactivation had been accomplished during the prepulse. The data were normalised and plotted against the voltage of the inactivating prepulse (circles). Errors due to series resistance are insignificant because currents at the end of the prepulse never exceeded 1.2 nA (corresponding to a worst error of 2.4 mV). Although currents during the test pulse are large, the test pulse is so strongly depolarising that even uncorrected voltages would still evoke maximum currents. Data for inactivation are for 11 cells, data for activation are for six cells. Error bars indicate one standard error of the mean (S.E.M.).

measured at the same membrane potential, so this method of measuring current activation did not require knowledge of the reversal potential. Activation curves of individual cells were fitted to a Boltzmann function of the form:

$$G(v)/G_{max} = 1/\{1 + \exp[(V_{50} - V)/s]\},$$

where $G(v)$ is conductance, G_{max} is maximum conductance, V is membrane potential, s is a slope factor, from which a half-activation potential (V_{50}) of 16.9±1.9 mV (mean ± S.E.M., N=6) and slope of 15.0±1.8 mV e^{-1} (mean ± S.E.M., N=6) were estimated after correction for predicted series resistance errors (assuming a series resistance of 4 MΩ and 50 % compensation).

The time course of the tail currents was best fitted by a double-exponential function. Both components had similar activation properties, suggesting that they represent a single current decaying with two time constants or two currents with similar activation ranges.

Inactivation

The rapidly inactivating component was isolated by digitally subtracting currents obtained during a depolarising step to +80 mV, which were preceded by a +20 mV conditioning pulse, from those obtained without the conditioning pulse. In 22 out of 26 cells, the resulting current inactivated with a time constant of 26.1±1.9 ms. In four cells, however, a better fit was obtained using a double-exponential function with time constants of 20.5±7.0 ms and 98.7±50.8 ms (means ± S.E.M.).

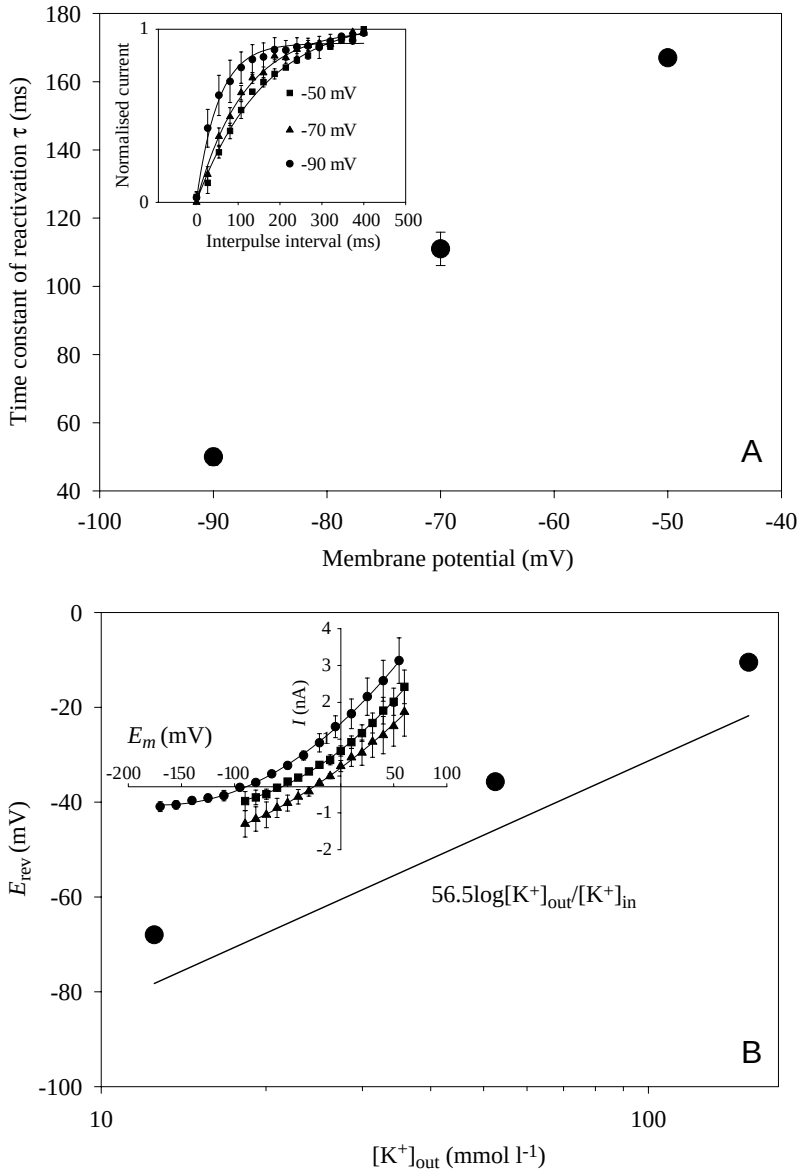

Fig. 5. (A) Voltage-dependence of the time course of recovery from inactivation of the rapidly inactivating current. Inset: the ratio of the peak amplitudes of currents elicited by two depolarising pulses to +100 mV, each of 100 ms duration, plotted against the interval between the two pulses at interpulse holding potentials of –90 mV (circles), –70 mV (triangles) and –50 mV (squares). *N*=5, error bars represent one standard error of the mean (S.E.M.). Time constants of recovery from inactivation measured from the data shown in the inset are plotted against the interpulse holding potential. *N*=5; error bars represent 1 S.E.M. (B) K^+-dependence of the outward currents. Inset: current–voltage curves generated using tail current amplitudes evoked by a return to –70 mV, from a potential of +120 mV, plotted against the voltages of a series of test potentials in perfusates containing 12 mmol l^{-1} (circles), 52 mmol l^{-1} (squares) or 152 mmol l^{-1} (triangles) K^+. Recording conditions as for Fig. 3. The intercepts on the voltage axis of the inset were plotted against the concentration of K^+ in the perfusate ($[K^+]_{out}$). The straight line represents the value of the K^+ equilibrium potential (E_{rev}) predicted by the equation E_K=56.5log($[K^+]_{out}/[K^+]_{in}$). $[K^+]_{in}$, intracellular $[K^+]$; E_m, membrane potential; *I*, current.

The voltage-dependence of inactivation was measured using a paired-pulse protocol in ASW. From a holding potential of –90 mV, the membrane was stepped to a range of potentials ranging from –120 to +60 mV for 200 ms and then immediately to +100 mV or +70 mV. The amplitudes of the peak current in response to the second pulse were plotted against the membrane potential of the preceding pulse and normalised (Fig. 4). Individual inactivation curves were fitted by Boltzmann functions with a mean half-inactivation potential of –35.4±3.0 mV and a slope of –9.5±0.6 mV e^{-1} (mean ± S.E.M., *N*=17). The range of values was –64.2 to –16.7 mV, although 14 of the 17 cells fell in the range –36.4 to –16.7 mV.

The time constant of inactivation of individual cells was measured during a depolarising pulse from –90 mV to +80 mV in ASW (12 mmol l^{-1} K^+), then again during perfusion with elevated $[K^+]$ (52 or 152 mmol l^{-1}). There was no significant difference between the time constants measured (12.6±5.2 ms for 152 mmol l^{-1} K^+ and 15.8±3.1 ms for 52 mmol l^{-1} K^+, *t*=0.921, d.f.=5, *P*=0.399, paired *t*-test). The rate of inactivation was also independent of the voltage of the conditioning pulse (data not shown).

Recovery from inactivation

To measure the time course of recovery from inactivation, two 100 ms depolarising steps to +100 mV from a holding potential of –70 mV were applied at successively diminishing intervals. The ratio of the peak amplitudes, after subtraction of the steady-state value, was plotted against the interval between the pulses (Fig. 5A, inset). Recovery from inactivation followed a single-exponential function, suggesting the existence of only one inactivated state. The rate of recovery was voltage-dependent (τ=50±2.5 ms at –90 mV, 111±4.9 ms at –70 mV and 167±8.3 ms at –50 mV, Fig. 5A) but was independent of the concentration of

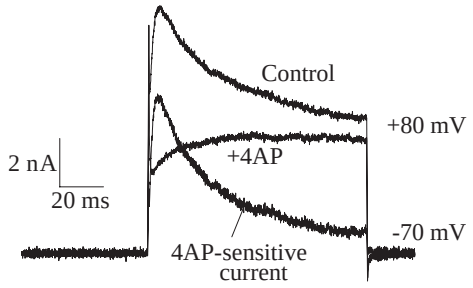

Fig. 6. The rapidly inactivating component of the K^+ currents is sensitive to 4-aminopyridine (4AP). The control trace was obtained in response to a membrane potential step from −70 mV to +80 mV in normal artificial sea water, while the 4AP trace was obtained 3 min after pressure-application of 10 mmol l^{-1} 4AP. The middle trace shows the difference current, the 4AP-sensitive current, which closely resembles the rapidly inactivating component of the outward current.

external K^+ (τ=124.4±18.4, N=4, for 12 mmol l^{-1} $[K^+]_{out}$, 98.7±14.4, N=4, for 52 mmol l^{-1} $[K^+]_{out}$, values that are not significantly different (one-way analysis of variance, P=0.554).

Ionic dependence of the outward currents

Tail-current protocols were used to determine the dependency of the reversal potential upon the external concentration of K^+. From a holding potential of −70 mV, the membrane potential was stepped to +100 mV for 10 ms to activate the currents and then to a series of potentials between −110 mV and +100 mV, at which point the tail currents were measured. This was performed in salines containing 12 mmol l^{-1}, 52 mmol l^{-1} and 152 mmol l^{-1} K^+. The reversal potentials measured in this way (−68.0 mV, −35.7 mV and −10.5 mV respectively, Fig. 5B, inset) were dependent upon the concentration of extracellular K^+ but differed from the equilibrium potentials for K^+ predicted from the concentrations of K^+ in the bathing medium and the pipette using the Nernst relationship (−78.3 mV, −45.9 mV and −21.8 mV, respectively, Fig. 5B). This suggests that these voltage-activated outward currents are mediated by K^+ and by some other, unidentified ionic species.

Pharmacology of the outward currents

Voltage-clamped cells were perfused for 3 min in K-ASW containing 10 mmol l^{-1} 4-aminopyridine (4AP). The currents evoked by a series of depolarising steps were subtracted from those previously obtained from the same cell in normal saline to reveal the 4AP-sensitive currents (Fig. 6). These currents were rapidly and completely inactivating with a time constant of 20.6±5.4 ms (mean ± S.E.M., N=5). In contrast, bath-application of tetraethylammonium (25 mmol l^{-1}) had no measurable effect on either rapidly inactivating or non-inactivating currents (N=11, data not shown). Outward currents were still recorded in all cells in the presence of 10 mmol l^{-1} Ba^{2+} in the bathing solution. Replacement of all the K^+ in the saline and in the pipette-filling solution with Cs^+ abolished most of the outward currents.

Discussion

We have shown that there are at least two K^+ currents present in cultured *Notoplana atomata* neurones: one rapidly activated (τ=0.9 ms) and inactivated (τ=26 ms), and the other also activated rapidly but showing no inactivation over 100 ms. Both currents activated at similar voltages (V_{50}=17 mV). The only characteristics that distinguished these two currents are the inactivation properties and sensitivity to 4AP. No other outward currents could be distinguished on the basis of the voltage-dependence of activation or inactivation, sensitivity to 4AP, barium or tetraethylammonium, or time to peak. Although we have not excluded the possibility that more than two current types exist in the cells from which we recorded, the simplest explanation of our results is that there are only two K^+ currents present. This suggests that variation in excitability properties is brought about by the differential expression of these two channel types in each neuronal phenotype. However, we cannot exclude the possibility that there are other populations of cells displaying other types of K^+ current that are not represented in our culture because of 'loss' during the culturing procedure.

The rate of inactivation of the rapidly inactivating current was independent of the concentration of external K^+, in contrast to *Polyorchis penicillatus* K^+ currents. This agrees with the suggestion of Grigoriev et al. (1999a) that K^+-dependent regulation of inactivation is a compensatory mechanism in organisms that have a paucity of glial cells. The *Notoplana atomata* brain is rich in glial cells (Koopowitz and Chien, 1974), which might provide an effective K^+ homeostatic mechanism.

Like most rapidly inactivating K^+ currents, the activation and inactivation curves of the currents we describe overlap. However, the values of activation threshold and half-activation are much more positive than for most K^+ currents reported to date and do not overlap with the resting potential of *in situ* neurones (Keenan and Koopowitz, 1984). In this respect, they resemble cloned K^+ channels from the mollusc *Aplysia californica* (Pfaffinger et al., 1991), the platyhelminth *Schistosoma mansoni* (Kim et al., 1995) and two cnidarian channels (Jegla et al., 1995). Thus, a class of rapidly inactivating K^+ channels with rightward-shifted activation curves is widespread among many invertebrates. This is probably not an adaptation of marine invertebrates to the high salt content of their extracellular fluids, since activation curves in muscle cells of *Schistosoma mansoni* (Day et al., 1993, 1995) and in lamina cells of the locust *Schistocerca gregaria* (Benkenstein et al., 1999) are also rightward-shifted, whereas those of some *Shaker* currents in *Aplysia californica* are not (Pfaffinger et al., 1991).

With a threshold of approximately −30 mV and a half-activation value of +17 mV, it is unlikely that either the rapidly inactivating or the slowly or non-inactivating component plays

a role in subthreshold integration, as suggested for $I_{K(A)}$ currents (Connor and Stevens, 1971). However, these currents are likely to be activated during action potentials since *Notoplana atomata* neurones *in situ* express overshooting action potentials whose peak in natural sea water may reach +50 mV with durations of 1–2 ms (Keenan and Koopowitz, 1984). Such depolarisations would be adequate to activate both K^+ currents almost fully. However, with a time constant of inactivation of approximately 26 ms and a time constant of recovery from inactivation of approximately 50 ms, inactivation is only likely to accumulate significantly at interspike intervals of less than approximately 50 ms, corresponding to frequencies greater than approximately $20\,s^{-1}$, suggesting that inactivation is an adaptation to high-frequency discharge. Multimodal interneurones of *Notoplana atomata* are capable of sustaining discharges of the order of $100\,s^{-1}$ (Keenan and Koopowitz, 1984). Within the mammalian *Shaker* superfamily of genes cloned to date, only the Kv3.1 and Kv3.4 families have rightward-shifted activation curves. Interestingly, recent evidence suggests that Kv3 channels may play a specific role in adapting neurones to high-frequency firing (Liu and Kaczmarek, 1998; Wang et al., 1998). The selective block of the inactivating current by 4AP and the ineffectiveness of tetraethylammonium as a blocking agent resemble findings from other cultured flatworm (*Bdelloura candida*) neurones (Blair and Anderson, 1993) and recall the lack of action of extracellular tetraethylammonium on spikes recorded from *Notoplana atomata* neurones *in situ*.

The slope factor ($15\,mV\,e^{-1}$) for activation of the rapidly inactivating current in *Notoplana atomata* neurones is comparable with the $15\,mV\,e^{-1}$ reported for cloned and $12\,mV\,e^{-1}$ for *in situ* K^+ channels from *Schistosoma mansoni* (Kim et al., 1995). It has been reported that the threshold and the slope factor are influenced by the total number of charges in the S4 segment of the channel (Liman et al., 1991; Logothetis et al., 1992, 1993; Papazian et al., 1991), although this is not always so (Smith-Maxwell et al., 1998). The gentle activation slope might therefore be explained by a reduction in the total nominal charge in the S4 segment of *Notoplana atomata* K^+ channels. Resolution of these questions awaits the cloning and functional expression of *Notoplana atomata* K^+ channels, which is in progress.

We thank the staff at Bamfield Marine Station for their assistance in providing ideal facilities for this study, which was supported by a NSERC research grant (A0419) to A.N.S.

References

Benkenstein, C., Schmidt, M. and Gewecke, M. (1999). Voltage-activated whole-cell K^+ currents in lamina cells of the desert locust *Schistocerca gregaria*. *J. Exp. Biol.* **202**, 1939–1951.

Blair, K. L. and Anderson, P. A. V. (1993). Properties of voltage-activated ionic currents in cells from the brains of the triclad flatworm, *Bdelloura candida*. *J. Exp. Biol.* **185**, 267–286.

Carranza, S., Baguna, J. and Riutort, M. (1997). Are the Platyhelminthes a monophyletic primitive group? An assessment using 18S rDNA sequences. *Mol. Biol. Evol*. **14**, 485–497.

Connor, J. A. and Stevens, C. F. (1971). Prediction of repetitive firing behaviour from voltage clamp data on an isolated neurone soma. *J. Physiol., Lond.* **213**, 31–53.

Day, T. A., Kim, E., Bennett, J. L. and Pax, R. A. (1995). Analysis of the kinetics and voltage-dependency of transient and delayed K^+ currents in muscle fibers isolated from the flatworm *Schistosoma mansoni*. *Comp. Biochem. Physiol.* **111**A, 79–87.

Day, T. A., Orr, N., Bennett, J. L. and Pax, R. A. (1993). Voltage-gated currents in muscle cells of *Schistosoma mansoni*. *Parasitol.* **106**, 471–477.

Faisst, J., Keenan, C. L. and Koopowitz, H. (1980). Neuronal repair and avoidance behavior in the flatworm, *Notoplana acticola*. *J. Neurobiol.* **11**, 483–496.

Field, K. G., Olsen, G. J., Lane, D. J., Giovannoni, S. J., Ghiselin, M. T., Raff, E. C., Pace, N. R. and Raff, R. A. (1988). Molecular phylogeny of the animal kingdom. *Science* **239**, 748–753.

Grigoriev, N. G., Spafford, J. D., Gallin, W. J. and Spencer, A. N. (1997). Voltage sensing in jellyfish *Shaker* K^+ channels. *J. Exp. Biol.* **200**, 2919–2926.

Grigoriev, N. G., Spafford, J. D. and Spencer, A. N. (1999a). The effects of level of expression of a jellyfish *Shaker* potassium channel: a positive potassium feedback mechanism. *J. Physiol., Lond.* **517**, 25–33.

Grigoriev, N. G., Spafford, J. D. and Spencer, A. N. (1999b). Modulation of jellyfish potassium channels by external potassium ions. *J. Neurophysiol*. **82**, 1728–1739.

Grigoriev, N. G., Spafford, J. D. and Spencer, A. N. (1999c). Residues in a jellyfish *Shaker*-like channel involved in modulation by external potassium. *J. Neurophysiol.* **82**, 1740–1747.

Hille, B. (1992). *Ionic Channels of Excitable Membranes*. Sunderland, MA: Sinauer.

Jegla, T., Grigoriev, N., Gallin, W. J., Salkoff, L. and Spencer, A. N. (1995). Multiple *Shaker* potassium channels in a primitive metazoan. *J. Neurosci.* **15**, 7989–7999.

Katayama, T., Nishioka, M. and Yamamoto, M. (1996). Phylogenetic relationships among turbellarian orders inferred from 18S rDNA sequences. *Zool. Sci*. **13**, 747–756.

Keenan, L. and Koopowitz, H. (1984). Ionic bases of action potentials in identified flatworm neurones. *J. Comp. Physiol.* A **155**, 197–208.

Keenan, L., Koopowitz, H. and Bernardo, K. (1979). Primitive nervous systems: action of aminergic drugs and blocking agents on activity in the ventral nerve cord of the flatworm *Notoplana acticola*. *J. Neurobiol.* **10**, 397–407.

Kim, E., Day, T. A., Bennett, J. L. and Pax, R. A. (1995). Cloning and functional expression of a *Shaker*-related voltage-gated potassium channel gene from *Schistosoma mansoni* (Trematoda: Digenea). *Parasitol.* **110**, 171–180.

Koopowitz, H., Bernardo, K. and Keenan, L. (1979a). Primitive nervous systems: electrical activity in ventral nerve cords of the flatworm, *Notoplana acticola*. *J. Neurobiol.* **10**, 367–381.

Koopowitz, H. and Chien, P. (1974). Ultrastructure of the nerve plexus in flatworms. I. Peripheral organization. *Cell Tissue Res.* **155**, 337–351.

Koopowitz, H., Keenan, L. and Bernardo, K. (1979b). Primitive nervous systems: electrophysiology of inhibitory events in flatworm nerve cords. *J. Neurobiol.* **10**, 383–395.

Koopowitz, H., Silver, D. and Rose, G. (1975). Neuronal plasticity

and recovery of function in a polyclad flatworm. *Nature* **256**, 737–738.

Koopowitz, H., Silver, D. and Rose, G. (1976). Primitive nervous systems. Control and recovery of feeding behavior in the polyclad flatworm, *Notoplana acticola*. *Biol. Bull.* **150**, 411–425.

Liman, E. R., Hess, P., Weaver, F. and Koren, G. (1991). Voltage-sensing residues in the S4 region of a mammalian K^+ channel. *Nature* **353**, 752–756.

Liu, S. Q. and Kaczmarek, L. K. (1998). Depolarization selectively increases the expression of the Kv3.1 potassium channel in developing inferior colliculus neurons. *J. Neurosci.* **18**, 8758–8769.

Logothetis, D. E., Kammen, B. F., Lindpaintner, K., Bisbas, D. and Nadal-Ginard, B. (1993). Gating charge differences between two voltage-gated K^+ channels are due to the specific charge content of their respective S4 regions. *Neuron* **10**, 1121–1129.

Logothetis, D. E., Movahedi, S., Satler, C., Lindpaintner, K. and Nadal-Ginard, B. (1992). Incremental reductions of positive charge within the S4 region of a voltage-gated K^+ channel result in corresponding decreases in gating charge. *Neuron* **8**, 531–540.

Papazian, D. M., Timpe, L. C., Jan, Y. N. and Jan, L. Y. (1991). Alteration of voltage-dependence of *Shaker* potassium channel by mutations in the S4 sequence. *Nature* **349**, 305–310.

Pfaffinger, P. J., Furukawa, Y., Zhao, B., Dugan, D. and Kandel, E. R. (1991). Cloning and expression of an *Aplysia* K^+ channel and comparison with native *Aplysia* K^+ currents. *J. Neurosci.* **11**, 918–927.

Ruiz-Trillo, I., Riutort, M., Littlewood, D. T., Herniou, E. A. and Bagun, J. (1999). Acoel flatworms: earliest extant bilaterian metazoans, not members of platyhelminthes. *Science* **283**, 1919–1923.

Smith-Maxwell, C. J., Ledwell, J. L. and Aldrich, R. W. (1998). Role of the S4 in cooperativity of voltage-dependent potassium channel activation. *J. Gen. Physiol.* **111**, 399–420.

Turbeville, J. M., Field, K. G. and Raff, R. A. (1992). Phylogenetic position of phylum Nemertini, inferred from 18S rRNA sequences: molecular data as a test of morphological character homology. *Mol. Biol. Evol.* **9**, 235–249.

Valentine, J. W., Jablonski, D. and Erwin, D. H. (1999). Fossils, molecules and embryos: new perspectives on the Cambrian explosion. *Development* **126**, 851–859.

Wang, L. Y., Gan, L., Forsythe, I. D. and Kaczmarek, L. K. (1998). Contribution of the Kv3.1 potassium channel to high-frequency firing in mouse auditory neurones. *J. Physiol., Lond.* **509**, 183–194.